Semiconductor Physics, Quantum Electronics & Optoelectronics, 2015. V. 18, N 1. P. 20-25.
doi: 10.15407/ spqeo18.01.020

PACS 81.05.Dz, 81.05.Rm, 81.07.St, 81.16.Be

Zinc oxide nanoparticles fabricated in the porous silica matrix by the sublimation method

G.Yu. Rudko[1], S.A. Kovalenko[1], E.G. Gule[1], V.V. Bobyk[2], V.M. Solomakha[2], A.B. Bogoslovskaya[1]
[1]V. Lashkaryov Institute of Semiconductors Physics, NAS of Ukraine
45, prospect Nauky, 03028 Kyiv, Ukraine; e-mail: g.yu.rudko@gmail.com.
[2]L. Pisarzhevskii Institute of Physical Chemistry, NAS of Ukraine
31, prospect Nauky, 03028 Kyiv, Ukraine

Abstract. The nanocomposite – nanoporous silica (SBA-16) containing ZnO quantum dots – was fabricated by the sublimation method. This novel route of synthesizing ZnO nanoparticles implies physical sorption of zinc acetylacetonate precursor into the matrix pores from the gaseous phase, hydrolysis of the precursor, and thermal decomposition of the product with formation of ZnO nanoclusters directly inside the pores. The nanocomposite was characterized by XRD, nitrogen adsorption-desorption isotherms, and photoluminescence spectroscopy methods. We observed the blue shift of the ultraviolet luminescence of nanocomposite as compared to the luminescence of ZnO nanopowder as well as the decrease of the linewidth of the ultraviolet luminescence line, which points to the encapsulation of ZnO nanoparticles in the silica pores and narrowing of their size distribution.

Keywords: ZnO nanoparticles, synthesis, nanoporous silica, luminescence.

Manuscript received 22.09.14; revised version received 19.11.14; accepted for publication 19.02.15; published online 26.02.15.

1. Introduction

New generation of composite materials – nanocomposites – has attracted great interest due to their potential impact in many areas such as electronics, photonics, catalysis, and sensing. For example, the composites containing semiconductor nanoparticles are the prospective candidates for future photonic and optoelectronic devices, e.g., the materials based on wide band gap semiconductors are promising for optoelectric devices operating in blue and ultraviolet (UV) ranges. Zinc oxide (ZnO) has shown a considerable potential as the starting material for fabrication of such composites[1].

ZnO is the II–VI group semiconductor with the band gap 3.37 eV at room temperature [2]. Low-dimensional nanocrystalline ZnO materials in the form of powders [3, 4], thin films [5-7], nanoparticles in colloids [8-12] received considerable attention in recent years due to observation of quantum confinement effects. An important issue for the study and applications of ZnO nanoparticles is to obtain a stable sample, because nanoparticles usually tend to form aggregates; consequently, the nanostructural properties can be lost. The task of the stabilization of size and shape of nanoparticles can be fulfilled by inserting them into some inert matrix (confinement host). The inorganic molecular sieves can offer a suitable host for nanoscale

semiconductor particles because they have uniform pore size distribution, high surface area and volume. Starting with the first reports on the synthesis of M41S, a whole family of nanoporous molecular sieves appeared [13,14]. They have different morphology, size and arrangement of pores, therefore, silica matrices provide a possibility to obtain the ordered arrays of ZnO quantum dots with different ordering types, which can be also interesting when making photonic crystals.

We have focused here on the representative of the SBA family of sieves – SBA-16. The molecular sieves of the SBA family have thicker walls than MCM materials. Therefore, SBA porous materials are more thermally and mechanically stable than materials of the MCM family [15]. Moreover, the surfactant that is used for the synthesis of these materials is nontoxic, biodegradable, and inexpensive [16]. These properties make SBA sieves an attractive host for nanoparticles. The particular representative of the SBA family used here – SBA-16 – is considered to be a very interesting mesostructure due to arrangement of mesopores into a cubic structure corresponding to the *Im*3*m* space group.

All the above advantages of the mesoporous silica molecular sieves for nanocomposites caused the extensive studies of zinc oxide incorporation into these materials. As a result, numerous methods for fabrication of nanocomposites were developed. By variation of zinc precursors, post-synthetical modifying treatments, and sequences of zinc oxide introducing into the pores, the ZnO particles different by size, shape and localization in the pores were obtained [17-20]. Here, we present the studies of zinc oxide/SBA-16 nanocomposites fabricated by the new sublimation method.

2. Experimental

2.1. Synthesis of SBA-16

Mesoporous silica SBA-16 is the representative of the SBA family of molecular sieves that can be synthesized using the Pluronic F127 surfactant as a template [21, 22]. Pluronic F127 is a three-block copolymer $EO_{106}PO_{70}EO_{106}$ (here: EO denotes the hydrophilic groups of ethelene oxide, PO denotes the hydrophobic groups of propilene oxide). We synthesized mesoporous silica SBA-16 analogously to the procedure outlined earlier in [23]: 0.57 g of Pluronic F-127 were dissolved in 26 ml of water and 4.87 g of concentrated HCl (37%); afterwards 2.6 ml of tetraethylorthosilicate (TEOS) were gradually added to the above solution at permanent stirring in the magnetic mixer at 60 ºC. The stirring lasted for 24 hours at the same temperature. The molar ratio of the components in the starting mixture of reactants was: 1 TEOS:0.004 F-127:4.2 HCl:119 H_2O. All the chemicals were analytical-grade reagents and were used without further purification.

The resulting product was further hydrothermally treated at 100 ºC during 24 hours. The solid component was then filtered out, washed in distilled water, and dried at 100 ºC. The remaining surfactant was removed by calcination at 550 ºC during 4-5 hours in air (the heating rate was 2 ºC/min). SBA-16 obtained in such a manner is a sieve of cubic symmetry (*Im*3*m*). Some textual properties are listed in Table.

Table. Textual properties of SBA-16 and ZnO/SBA-16 samples.

Sample	ZnO content (mass.%)	SBET (m^2/g)	*d* (Å) of the cavity	*V* (cm^3/g) of the micropores
SBA-16	0	589	71	0.045
ZnO/SBA-16	12.4	294	53	0.02

2.2. Loading of zinc oxide into SBA-16

ZnO-containing nanocomposite was fabricated on the base of porous silica matrix SBA-16 by using the sublimation method. The method implies sorption of gaseous zinc acetylacetonate precursor into the pores of the host with consequent hydrolysis, decomposition of the hydrolysis products and formation of ZnO. Taking into account that high surface area of molecular sieves mainly originates from the pore system, while relatively small part is provided by the external surface, we expected that formation of ZnO nanocrystals should mainly occur in the pores. Moreover, as the sorption process is rather slow, it is quite probable that distribution of the precursor in the pores could be sufficiently homogeneous and, finally, dispersion of the sizes of ZnO nanoclusters obtained after hydrolysis will reproduce dispersion of pore sizes.

The procedure of SBA-16 loading with ZnO was carried out in a two-chamber evacuated vessel. One chamber was filled with SBA-16 and the other one with zinc acetylacetonate. At first, the chamber with SBA-16 was heated up to 350 ºC and the material was calcined for two hours under evacuation. After cooling down to room temperature, the two-chamber vessel was soldered up, and the two materials were mixed. By heating the mixture up to 95 ºC, zinc acetylacetonate was sublimated. To ensure the precursor sorption into the matrix channels, heating lasted for two days. Zinc oxide was formed inside the pores via hydrolysis of zinc acetylacetonate in the water vapor and calcination at 550 ºC during three hours.

2.3. Characterization methods

The powder XRD patterns were recorded by a DRON-3M diffractometer using the CuKα radiation source, λ = 1.542 Å.

The surface area was measured by the nitrogen adsorption–desorption method. The N_2 adsorption-desorption isotherms were obtained in Sorptomatic 1990 at 77 K under continuous adsorption conditions. The Brunauer–Emmett–Teller (BET) specific surface area of the sample was calculated using adsorption data. The pore size distribution curves were calculated from the

analysis of the adsorption branch of the isotherm employing the Barrett–Joyner–Halenda (BJH) algorithm.

Room temperature photoluminescence spectra were recorded with the MDR-23 spectrometer with PMP-100 photomultiplier as a detector. The N_2-laser (λ = 337 nm) was used as the excitation source.

3. Results and discussion

3.1. X-ray diffraction results

Typical small-angle X-ray diffraction patterns for pure SBA-16 porous silica (*1*) and nanocomposite material (*2*) are shown in Fig. 1. These reveal only one diffraction peak at 2θ of about 1°. Observation of this diffraction peak points to the presence of the periodically organized mesoporous structure with regular repetition of the pore diameter. It is seen that the position of the reflection peak is the same both for pure SBA-16 and ZnO-containing composite, and the intensity of the peak does not change essentially after introduction of ZnO into the porous matrix. It proves that the ZnO-containing matrix maintains the same order, i.e. keeps the same size of the unit cell upon ZnO loading and subsequent treatments. Thus, introduction of ZnO does not affect the mesoscopic order in the host.

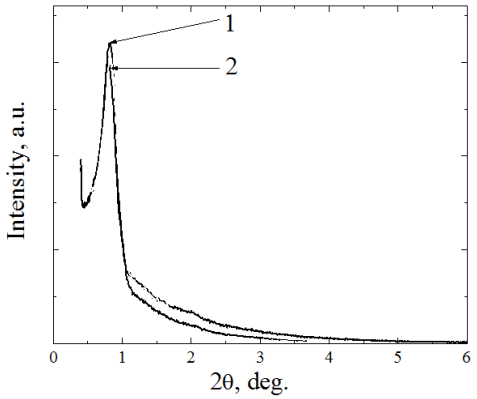

Fig. 1. Small angle XRD patterns of the pure SBA-16 porous silica (*1*) and ZnO-containing nanocomposite material (*2*).

We have also studied the XRD patterns of ZnO-containing nanocomposite material within the 10…70° range and, for comparison, the XRD patterns of bulk ZnO and nanosized ZnO powder. The results are presented in Fig. 2.

It is seen that the reflexes characteristic for the wurtzite structure can be observed in the patterns of both bulk ZnO (curve *1*) and ZnO nanopowder (curve *2*). The reflexes of the nanopowder are less intense and wider, which is typical for nanosize materials. The composite material shows no characteristic peaks of the wurtzite ZnO structure (curve *3*). This observation correlates with the data of other authors on SBA-15 based composites [24, 25] and can be interpreted either by the absence of ZnO in the material or as the presence of very small ZnO clusters formed inside the pores. We have ruled out the former interpretation by application of the chemical analysis method. The results obtained using this method are shown in Table. It is seen that ZnO has been successfully loaded into SBA host. The content of ZnO in the material is as large as 12.4 mass.%. Therefore, the absence of ZnO-like peaks in curve *3* together with chemical analysis results indicate that ZnO is well dispersed within the pores and there are no large (bulk) oxide particles formed outside the pore structure.

3.2. Inner surface and pores volume

The pore characteristics of pure and ZnO-loaded SBA-16 were obtained from the analysis of nitrogen adsorption-desorption isotherms shown in Fig. 3. The isoterms are all of the type IV classification, which is characteristic of adsorption on mesoporous materials [26].

The parameters calculated from these data are listed in Table. The characteristic sizes and the pore volume of pure SBA-16 are in good agreement with the other literature data available [27]. The decrease of BET surface area, average pore diameters and pore volumes with ZnO loading indicates that ZnO clusters should be confined in the pores of SBA-16.

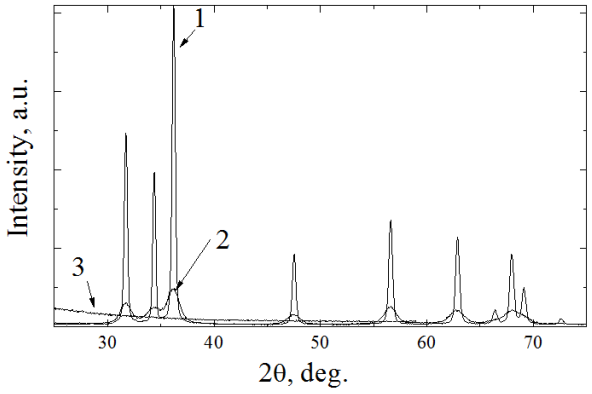

Fig. 2. XRD patterns of bulk ZnO (*1*), nanosize powder of ZnO (*2*), and nanocomposite ZnO/SBA-16 (*3*).

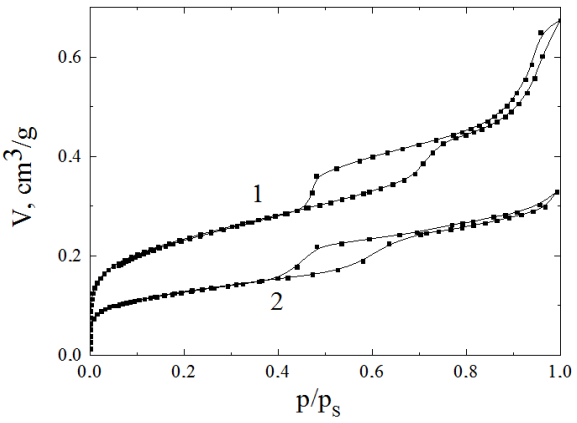

Fig. 3. Nitrogen adsorption–desorption isotherms for pure SBA-16 (*1*) and ZnO-containing nanocomposite (*2*).

3.3. PL results

Fig. 4 shows the normalized room-temperature PL spectra of ZnO/SBA-16 nanocomposite (*1*) and ZnO nano-powder (*2*). The insert shows the real-scale photoluminescence spectra of ZnO/SBA-16 (*1*), nano-ZnO (*2*) and unloaded SBA-16 (*3*). It is seen that the unloaded molecular sieve (spectrum *3* in the insert) does not emit light in the spectral range studied, thus, it cannot mask the emission of ZnO that is introduced into the silica matrix. The emissions of ZnO-containing nanocomposite and ZnO nanoparticles (spectra *1* and *2*, respectively) show some similarities and differences. Specifically, the spectra of both materials exhibit a sharp peak within the ultraviolet range (380…390 nm), while only in the spectrum of nano-powder zinc oxide the emission at longer wavelengths is seen.

These spectroscopic features are related to those observed in bulk ZnO. It is known that in bulk ZnO the peak within the ultraviolet range is usually ascribed to the near-band-edge transitions, including recombination of electron-hole pairs, free excitons, and bound excitons. The green emission (centered near 550 nm) in undoped ZnO is commonly referred to structural defects, such as zinc vacancy, oxygen vacancy, interstitial zinc, interstitial oxygen, and antisite oxygen [29-35]. This defect-related emission is a competing recombination channel for the UV emission, and, thus, is supposed to be unfavorable for applications of ZnO in the UV light emitting devices. The absence of visible emission in the spectra of composite material (spectrum *1* in Fig. 4) implies that ZnO particles have a very low defect density and good optical quality, while the quality of ZnO crystallites in the powder samples is close to that of ZnO films.

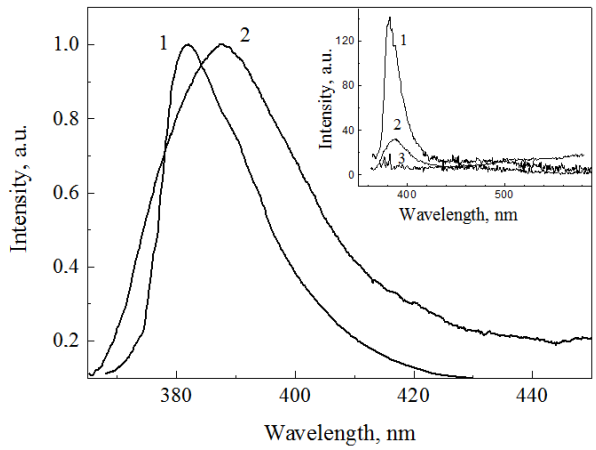

Fig. 4. Normalized room temperature photoluminescence spectra of ZnO/SBA-16 (*1*) and nano-ZnO (*2*). The PL excitation source – N_2-laser (λ = 337 nm). The insert shows the real-scale photoluminescence spectra of ZnO/SBA-16 (*1*), nano-ZnO (*2*) and unloaded SBA-16 (*3*).

An important feature in the spectra in Fig. 4 is the shift of the ultraviolet PL maximum of ZnO-SBA-16 nanocomposite (λ = 381.8 nm) as compared to that of ZnO nanopowder (λ = 387.6 nm). This observation points to the encapsulation of ZnO particles in the mesopores of SBA-16. The observed spectral position of the ultraviolet peak is also blue-shifted as compared to that observed in the PL spectra of ZnO/SBA-15 [24]. The latter composite was also obtained by using the solvent-free method, but of a different kind. Thus, one can assume that our sublimation method provides ZnO particles of smaller average sizes than the method [24].

It should be also noted that the full width at half maximum (FWHM) of the ultraviolet peak in the spectrum of composite is smaller than FWHM of the corresponiding peak of ZnO powder. The cause of peak narrowing is probably related to more narrow distribution of the particles sizes in silica matrix as compared to that in the powder. The higher homogeneity of size distribution can be caused by the homogeneity of distribution by pores sizes as well as slow sublimation of zinc acetilacetonate during loading the SBA matrix.

Thus, the PL results are in good agreement with those of X-rays diffraction and nitrogen adsorption-desorption isotherms methods, and demonstrate that the method proposed provides good luminescent material.

4. Conclusions

We have reported on the successful synthesis of the SBA-16-based nanocomposite containing ZnO quantum dots by using the sublimation method. The ZnO quantum dots were formed directly inside the matrix pores by hydrolysis and thermal decomposition of physisorbed zinc acetilacetonate precursor. All chemical and thermal treatments during the procedure of ZnO nanoparticles formation did not change the intrinsic structure of the SBA-16 matrix. The presence of ZnO nanoparticles in the matrix was proved by changes in the surface and volume of pores as well as by observation of characteristic ZnO photoluminescence bands. The observed blue shift of the ultraviolet luminescence band in nanocomposites as compared to the corresponding band of ZnO nanopowder demonstrated larger influence of carriers confinement in the ZnO quantum dots.

Aknowledgements

This work was partially supported by the State Fund for Fundamental Researches (Ukraine), project 49-02-14 (У).

References

1. A. Kołodziejczak-Radzimska, T. Jesionowski, Zinc oxide-from synthesis to application: a review // *Materials*, **7**, p. 2833-2881 (2014).

2. Z.H. Wang, Zinc oxide nanostructures: growth, properties and applications // *J. Phys.: Condens. Matter*, **16**, p. R829-R858 (2004).
3. S.A. Studenikin, N. Golego, M. Cocivera, Fabrication of green and orange photoluminescent, undoped ZnO films using spray pyrolysis // *J. Appl. Phys.* **84**(4), p. 2287-2294 (1998).
4. A. Ortíz, M. Garcia, J.C. Alonso et al., Photoluminescent characteristics of lithium-doped zinc oxide films deposited by spray pyrolysis // *Thin Solid Films*, **293**, p. 103-107 (1997).
5. R.M. Nyffenegger, B. Craft, M. Shaaban, S. Gorer, G. Erley, R.M. Penner, A hybrid electrochemical/chemical synthesis of zinc oxide nanoparticles and optically intrinsic thin films // *Chem. Mater*. **10**, p. 1120-1129 (1998).
6. M. Izaki, T. Omi, Characterization of transparent zinc oxide films prepared by electrochemical reaction // *J. Electrochem.* **144**(6), p. 1949-1952 (1997).
7. C.M. Mo, Y.H. Li, Y.S. Liu, Y. Zhang, L.D. Zhang, Enhancement effect of photoluminescence in assemblies of nano-ZnO particles/silica aerogels // *J. Appl. Phys*. **83**, p. 4389-4391 (1998).
8. U. Koch, A. Fojtik, H. Weller, A. Henglein, Photochemistry of semiconductor colloids. Preparation of extremely small ZnO particles, fluorescence phenomena and size quantization effects // *Chem. Phys. Lett.* **122**, p. 507-510 (1985).
9. M. Haase, H. Weller, A. Henglein, Photochemistry and radiation chemistry of colloidal semiconductors. 23. Electron storage on ZnO particles and size quantization // *J. Phys. Chem.* **92**, p. 482-487 (1988).
10. D.W. Bahnemann, C. Kormann, M.R. Hoffmann, Preparation and characterization of quantum size zinc oxide: A detailed spectroscopic study // *J. Phys. Chem.* **91**, p. 3789-3798 (1987).
11. P. Hoyer, H. Weller, Size-dependent redox potentials of quantized zinc oxide measured with an optically transparent thin layer electrode // *Chem. Phys. Lett.* **221**, p. 379-384 (1994).
12. L. Spanhel, M.A. Anderson, Semiconductor clusters in the sol-gel process: Quantized aggregation, gelation, and crystal growth in concentrated ZnO colloids // *J. Am. Chem. Soc.* **113**, p. 2826-2833 (1991).
13. C.T. Kresge, M.E. Leonowicz, W.J. Roth, J.C. Vartuli, J.S. Beck, Ordered mesoporous molecular sieves synthesized by a liquid-crystal template mechanism // *Nature*, **359**, p. 710-712 (1992).
14. J.S. Beck, J.C. Vartuli, W.J. Roth et al., A new family of mesoporous molecular sieves prepared with liquid crystal templates // *J. Am. Chem. Soc.* **114**, p. 10834-10843 (1992).
15. K. Cassiers, T. Linssen, M. Mathieu et al., A detailed study of thermal, hydrothermal, and mechanical stabilities of a wide range of surfactant assembled mesoporous silicas // *Chem. Mat.* **14**, p. 2317-2324 (2002).
16. H. Sun, Q. Tang, Yu Du, X. Liu, Yu. Chen, Ya.Yang, Mesostructured SBA-16 with excellent hydrothermal, thermal and mechanical stabilities: Modified synthesis and its catalytic application // *J. Colloid and Interface Sci.* **333**, p. 317-323 (2009).
17. B. Yao, Hu. Shi, Hu. Bi, L. Zhang, Optical properties of ZnO loaded in mesoporous silica // *J. Phys.: Condens. Matter*, **12**, p. 6265-6270 (2000).
18. C. Bouvy, W. Marine, B.-L. Su, ZnO/mesoporous silica nanocomposites prepared by the reverse micelle and the colloidal methods: Photoluminescent properties and quantum size effect // *Chem. Phys. Lett.* **438**(1-3), p. 67-71 (2007).
19. P.B. Lihitkar, S. Violet, M. Shirolkar et al., Confinement of zinc oxide nanoparticles in ordered mesoporous silica MCM-41 // *Mater. Chem. and Phys.* **133**, p. 850-856 (2012).
20. K. Sowri Babu, A. Rama Chandra Reddy, Ch. Sujatha, K. Venugopal Reddy, N. Venkatathri, Structural and optical properties of ZnO nanoclusters supported on mesoporous silica // *Optoelectron. and Adv. Mater.* – Rapid Communs. **5**(9), p. 943-947 (2011).
21. M. Kruk, M. Jaroniec, Characterization of MCM-48 silicas with tailored pore sizes synthesized via a highly efficient procedure // *Chem. Mater.* **12**, p. 1414-1421 (2000).
22. D. Zhao, J. Feng, Q. Huo et al., Triblock copolymer syntheses of mesoporous silica with periodic 50 to 300 angstrom pores // *Science*, **279**, p. 548-552 (1998).
23. F. Kleitz, D.N. Liu, G.M. Anilkumar, I. S. Park, L.A. Solovyov, A.N. Shmakov, R. Ryoo, Large cage face-centered-cubic *Fm*3*m* mesoporous silica: Synthesis and structure // *J. Phys. Chem. B*, **107**(51), p. 14296-14300 (2003).
24. Q. Jiang, Z.Y. Wu, Y.M. Wang, Y. Cao, C.F. Zhu, J.H. Zhu, Fabrication of photoluminescent ZnO/SBA-15 through directly dispersing zinc nitrate into the as-prepared mesoporous silica occluded with template // *J. Mater. Chem.* **16**, p. 1536-1542 (2006).
25. K. Dimos, I.B. Koutselas, M.A. Karakassides, Synthesis and characterization of ZnS nanosized semiconductor particles within mesoporous solids // *J. Phys. Chem. B*, **110**, p. 22339-22345 (2006).
26. S. Brunauer, L.S. Deming, W.S. Deming, E. Teller, On a theory of the van der Waals adsorption of gases // *J. Am. Phys. Soc.* **62**, p. 1723-1732 (1940).
27. R.M. Grudzien, B.E. Grabicka, M. Jaroniec, Effective method for removal of polymeric template from SBA-16 silica combining extraction and temperature-controlled calcinations // *J. Mater. Chem*. **16**, p. 819-823 (2006).
28. Z.K. Tang, G.K.L. Wong, P. Yu, M. Kawasaki, A. Ohtomo, H. Koinuma, Room-temperature ultraviolet laser emission from self-assembled ZnO microcrystallite thin films // *Appl. Phys. Lett*. **72**, p. 3270-3272 (1998).

29. Y.C. Kong, D.P. Yu, B. Zhang, W. Fang, S.Q. Feng, Ultraviolet-emitting ZnO nanowires synthesized by a physical vapor deposition approach // *Appl. Phys.Lett.* **78**, p. 407-409 (2001).
30. F. Hamdani, A. Botchkarev, W. Kim et al., Optical properties of GaN grown on ZnO by reactive molecular beam epitaxy // *Appl. Phys. Lett.* **70**, p. 467-469 (1997).
31. W.S. Shi, O. Agyeman, C.N. Xu, Enhancement of the light emissions from zinc oxide films by controlling the post-treatment ambient // *J. Appl. Phys.* **91**, p. 5640 (2002).
32. M.H. Huang, Y.Y. Wu, H. Feick, N. Tran, E. Weber, P.D. Yang, Catalytic growth of zinc oxide nanowires by vapor transport // *Adv. Mater.* 13, p. 113-116 (2001).
33. X.M. Sun, Z.X. Deng, Y.D. Li., Self-organized growth of ZnO single crystal columns array // *Chem. Phys.* **80**, p. 366-370 (2003).
34. Z. Fang, Yi. Wang, D. Xu, Yo. Tan, Xu.Liu, Blue luminescent center in ZnO films deposited on silicon substrates // *Opt. Mater.* **26**, p. 239-242 (2004).
35. N.O. Korsunska, L.V. Borkovska, B.M. Bulakh, L.Yu. Khomenkova, V.I. Kushnirenko, I.V. Markevich, The influence of defect drift in external electric field on green luminescence of ZnO single crystals // *J. Lumin.* **102-103**, p. 733-736 (2003).